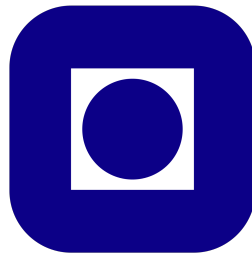

Sources of Ultra High Energy Cosmic Rays and Neutrinos



Henrik Døvre Andrews
Norwegian university of Science and Technology

April 24, 2024

Preface

Lorem ipsum dolor sit amet, consectetur adipiscing elit. Ut purus elit, vestibulum ut, placerat ac, adipiscing vitae, felis. Curabitur dictum gravida mauris. Nam arcu libero, nonummy eget, consectetur id, vulputate a, magna. Donec vehicula augue eu neque. Pellentesque habitant morbi tristique senectus et netus et malesuada fames ac turpis egestas. Mauris ut leo. Cras viverra metus rhoncus sem. Nulla et lectus vestibulum urna fringilla ultrices. Phasellus eu tellus sit amet tortor gravida placerat. Integer sapien est, iaculis in, pretium quis, viverra ac, nunc. Praesent eget sem vel leo ultrices bibendum. Aenean faucibus. Morbi dolor nulla, malesuada eu, pulvinar at, mollis ac, nulla. Curabitur auctor semper nulla. Donec varius orci eget risus. Duis nibh mi, congue eu, accumsan eleifend, sagittis quis, diam. Duis eget orci sit amet orci dignissim rutrum.

Abstract

Lorem ipsum dolor sit amet, consectetur adipiscing elit. Ut purus elit, vestibulum ut, placerat ac, adipiscing vitae, felis. Curabitur dictum gravida mauris. Nam arcu libero, nonummy eget, consectetur id, vulputate a, magna. Donec vehicula augue eu neque. Pellentesque habitant morbi tristique senectus et netus et malesuada fames ac turpis egestas. Mauris ut leo. Cras viverra metus rhoncus sem. Nulla et lectus vestibulum urna fringilla ultrices. Phasellus eu tellus sit amet tortor gravida placerat. Integer sapien est, iaculis in, pretium quis, viverra ac, nunc. Praesent eget sem vel leo ultrices bibendum. Aenean faucibus. Morbi dolor nulla, malesuada eu, pulvinar at, mollis ac, nulla. Curabitur auctor semper nulla. Donec varius orci eget risus. Duis nibh mi, congue eu, accumsan eleifend, sagittis quis, diam. Duis eget orci sit amet orci dignissim rutrum.

Acknowledgments

I would like to thank my supervisor, Professor Foteini Oikonomou, for her guidance and help throughout this project. I would also like to thank my fellow students for their help and support. Balasubramaniam et al. 2021

List of Figures

1	The total energy density of the photon fields as a function radius from central engine.	12
2	The spectral energy density at distance R	12
3	Luminosity of the different components of the CSO that are close by the central engine. Missing synchrotron and IC part which is most prominent	12

List of Tables

1	Parameters used to determine the SED of the different regions.	11
---	--	----

1 Introduction

1. The motivation for looking for UHECRs and Neutrinos
2. What multimessenger astronomy can give us
3. The difficulty of knowing the sources of multimessengers
4. The possible source population
5. Outline

2 The ever-expanding Universe

To investigate sources very far away from an observer it is important to understand the influence this distance has on the desired observables. Therefore, in astrophysics and astronomy in general there are distances created to take into account the effects of an expanding Universe. This chapter draws heavily from Hogg 2000.

2.1 Cosmological parameters

A reasonable place to start is with the Hubble constant H_0 . This parameter sets the recession speed of a point at proper distance d and the current position via the relation $v = H_0 d$. The subscript 0 refers to the present epoch signifying that H_0 is not static but changes with time. The precise value of H_0 is quite debated, so it's commonly expressed in a parameterised form,

$$H_0 = 100 \frac{\text{km}}{\text{s}} \frac{1}{\text{Mpc}} h.$$

The parameter h is a dimensionless number that according to current knowledge can take the value between 0.5 to 0.8 reflecting the range of answers collected from recent work.

Beyond its basic definition, H_0 also allows for the derivation of two significant cosmic scales:

Hubble Time (t_H) : Defined as the inverse of H_0 , t_H provides an estimate of the age of the Universe. It sets a scale for the time since the Big Bang, assuming the Universe has been expanding at a constant rate. The equation $t_H = 1/H_0 \approx 14$ Billion years offers a way to approximate this expansion timescale.

Hubble Distance (D_H) : This is a measure of the distance. Calculated as $D_H = c/H_0 \approx 4.4$ Gly, where c is the speed of light, it represents a critical boundary in observational cosmology.

2.2 Shape of the Universe

The shape and expansion of the Universe are central themes in cosmology, but to model such one needs to define the structure of the Universe and its contents. In this report and many articles, the Universe is often explored through the lens of the flat Lambda Cold Dark Matter (Λ CDM) model. This model, widely accepted in contemporary cosmology, provides a framework for understanding the Universe's composition and its expansion dynamics by assuming as the name suggests no curvature and cold dark matter. In the Λ CDM model, two key parameters are important: the mass density of the Universe, ρ_0 , and the cosmological constant, Λ . These parameters, which evolve, are a part of defining the metric tensor in general relativity, thereby allowing us to model the curvature of the Universe based on its initial conditions. These parameters are often expressed as dimensionless variables:

$$\Omega_m = \frac{8\pi G \rho_0}{3H_0^2}$$

$$\Omega_\Lambda = \frac{\Lambda c^2}{3H_0^2}$$

Here, Ω_m represents the matter density parameter, encompassing both ordinary (baryonic) matter and dark matter. Ω_Λ , on the other hand, corresponds to the density parameter associated with the cosmological constant, which is often interpreted as dark energy.

In general, one has a third density parameter Ω_k which defines the curvature of space-time and the relationship between these parameters is expressed as:

$$\Omega_m + \Omega_\Lambda + \Omega_k = 1$$

In a flat Universe, one has $\Omega_k = 0$ and the Universe is dominated by dark energy and dark matter. The model used in this report and the papers used in the following chapters is the flat Λ CDM model where the parameters take the values of $\Omega_\Lambda = 0.7$ and $\Omega_m = 0.3$. These values align with current observational data.

2.3 Redshift

Redshift is defined as the fractional Doppler shift of emitting light. The Doppler effect is a known effect on different observables in the Universe where the relative motion of sources to observers will impact the observable. The redshift is quantified for a light source as

$$z = \frac{\nu_e}{\nu_o} - 1 = \frac{\lambda_o}{\lambda_e} - 1 \quad (1)$$

Here o refers to the observed quantity and e the emitted. Due to the expansion of the Universe the light emitted from a distant source will be increasingly redshifted the further away it is. In these scenarios the redshift serves as a distance measure, allowing us to deduce distances to faraway objects.

2.4 Comoving distance

Comoving distance is an important concept in cosmography, acting as a standard unit for various distance measurements in the Universe. This distance, often termed the line-of-sight distance for an observer on Earth, remains constant even as objects expand with the Hubble flow. To calculate the total comoving distance (D_c) to an object, one integrates the differential comoving distances (δD_c) along the line of sight, starting from redshift $z = 0$ to the object. This integration necessitates consideration of the Universe's parametric composition and the δD_c is expressed as

$$\delta D_c = \frac{D_H}{E(z)} dz, \quad (2)$$

where the function $E(z)$ is defined as

$$E(z) = \sqrt{\Omega_m(z+1)^3 + \Omega_k(1+z)^2 + \Omega_\Lambda}. \quad (3)$$

Here, $E(z)$ incorporates the density parameters previously discussed and the redshift z . It also relates to the Hubble constant observed by a hypothetical observer at redshift z , expressed as $H(z) = H_0 E(z)$.

One then calculates the comoving distance D_c from

$$D_c = D_H \int_0^z \frac{dz}{E(z)} \quad (4)$$

In addition to the line of sight, one can define the transverse comoving distance D_m . This distance relates two points in the night sky at the same redshift separated by an angle $d\theta$. The actual distance between them $d\theta D_m$ will then vary depending on the curvature of the Universe. This relationship is summarized in

the following equation which accounts for different geometries,

$$D_m = \begin{cases} D_h \frac{1}{\sqrt{\Omega_k}} \sinh\left(\frac{\sqrt{\Omega_k} D_c}{D_H}\right) & \text{if } \Omega_k > 0 \\ D_c & \text{if } \Omega_k = 0 \\ D_h \frac{1}{\sqrt{|\Omega_k|}} \sin\left(\frac{\sqrt{|\Omega_k|} D_c}{D_H}\right) & \text{if } \Omega_k < 0 \end{cases}$$

The different cases correspond to hyperbolic, flat, and spherical geometry respectively. The true nature of the Universe is still unknown, but recent observations indicate a flat Universe.

2.5 Luminosity distance

The luminosity distance D_l is defined through the relation between the bolometric flux F of a source and its bolometric luminosity L . Bolometric flux is the energy received per unit of time per unit area without any obscuration, while bolometric luminosity is the total energy emitted per unit of time. The luminosity distance is defined as

$$D_l = \sqrt{\frac{L}{4\pi F}} \quad (5)$$

It is related to the transverse comoving distance via

$$D_l = (1 + z)D_m. \quad (6)$$

If one wants to calculate the spectral flux/ differential flux one needs to take into account a correction. This correction comes from the fact that one is viewing a redshifted object. The object is emitting in a different band than observed. The spectrum of the differential flux F_ν is related to the spectral luminosity via

$$F_\nu = (1 + z) \frac{L_{(1+z)\nu}}{L_\nu} \frac{L_\nu}{4\pi D_l^2}. \quad (7)$$

All these equations listed help include the effects of an expanding Universe when astronomers study distant objects and their properties.

3 Compact symmetric objects

1. Introduction to CSOs
2. What is a CSO
3. more on the structure of CSOs
4. The different types of CSOs
5. The prevalence of CSOs
6. CSO as candidates for UHECRs and neutrinos
 - (a) Hillas criterion, Flux of X-ray compared to diffuse flux of UHECRs and neutrinos
 - (b) Kinetic jet power
 - (c) Timescale analysis

Introduction to CSOs

In regards to other types of AGN CSO or Compact symmetric objects are similar to Seyfert Galaxies. They are characterized by their small projected size which in Kiehlmann et al. 2023 is described by being less than one kiloparsec and having symmetric radio emissions on both sides of the central activity. They are also in the group of Jetted AGN, but are distinguish from other sources of jetted AGN because the jet is non-relativistic, and there is a lack of relativistic boosting. In the paper and subsequent papers by Kiehlmann et al. 2023 and their group there were some overlap in classification of some sources, where some sources were classified as CSOs when in reality they were not. This was due to the fact that one overlooked two "new" properties of AGN that will also be important in this paper. CSOs are also characterized by low variability in radio and low apparent speed along the jet.

3.1 Structure of CSOs

This section will try to constate the structure of CSOs.

3.2 Timescale analysis of CSOs

In this section one will investigate the relevant timescales of a CSO and understand which processes are dominant and to the maximum energy one could expect of an escaping proton. First we begin by determining the acceleration timescale of a proton undergoing second order fermi acceleration. The acceleration timescale is given by the equation

$$t_{acc} = \frac{\eta \epsilon}{ZeBc} \quad (8)$$

where η is the efficiency of the acceleration process with the most efficient acceleration harbouring the value $\eta \approx (1 - 10)$, ϵ is the energy of the particle, Z is the charge of the particle, e is the elementary charge, B is the magnetic field strength and c is the speed of light. The value used for the magnetic field strength is $B = 10^{-2}$ G, which is the value found in Bronzini et al. 2024 based on the equipartition argument in the radio lobes. This value would need to change if investigating different regions, but in this analysis one has most data on the radio lobes. The value of η is taken to be 1, which is the most efficient acceleration process.

The promising feature for CSOs is the low variability. In most studies one uses the variability to determine the size of the emission region. In the case of CSOs one can use the size of the radio lobes to determine

the size of the emission region or the estimated variability of the source which according to Kiehlmann et al. 2023 is on the order of years to decades. This gives us an emission region of $R \sim 10^{18}$ cm.

The next timescale that is still quite trivial to introduce is the synchrotron cooling timescale. This is given by the equation

$$t_{sync} = \frac{6\pi m_p^4 c^3}{\sigma_T m_e^2 B^2 E} \quad (9)$$

where m_p is the proton mass, m_e is the electron mass, σ_T is the Thompson cross section, B is the magnetic field strength, E is the energy of the particle and c is the speed of light. To be precise this is the synchrotron loss timescale for protons and not electrons.

The last timescale used in this analysis is the pion production timescale. This is the timescale for a proton to interact with a photon and produce a pion. This equation is more convoluted than the previous ones since one needs to include the relevant photon fields the proton might experience. The equation is given by

$$t_{pr}^{-1}(\varepsilon_p) = \frac{c}{2\gamma_p^2} \int_{\varepsilon_{th}}^{\infty} d\varepsilon \sigma_{pr}(\varepsilon) k_p(\varepsilon) \int_{\varepsilon/2\gamma_p}^{\infty} d\varepsilon' \varepsilon'^{-2} \frac{dn}{d\varepsilon'} \quad (10)$$

where ε_p is the energy of the proton, γ_p is the lorentz factor of the proton, ε_{th} is the threshold energy for the interaction, σ_{pr} is the cross section for the interaction, k_p is the photon field, and $dn/d\varepsilon$ is the differential photon density.

3.2.1 photon fields

In order to determine the photon fields we follow Ghisellini and Tavecchio 2009 which describe the photon fields surrounding a Blazar. The photon fields sperates into different contribution from the different regions of a classic AGN as discussed in section ... The different regions are the accretion disk, the broad line region, the torus and the x-ray corona.

Accretion disk: The photon field emerging from an accretion disk if calculated by assuming a black body spectrum at each ring of an Shakura-Sunyaev disk and summing up its contributions. The temperature of each ring in the disk is given by

$$T(R) = \left(\frac{3R_S L_d}{16\pi R^3 \eta \sigma_{SB}} \left(1 - \left(\frac{3R_S}{R} \right)^{\frac{1}{2}} \right) \right)^{\frac{1}{4}} \quad (11)$$

Each ring of the accretion disk is assumed to be at the same temperature and emitting as a black-body spectrum. By using this temperature one can use the black body spectrum of an object with temperature T to find the intensity:

$$I(\nu) = \frac{2h\nu^3}{c^2} \left(\frac{1}{\exp\left(\frac{h\nu}{k_B T}\right) - 1} \right) \quad (12)$$

By integrating the intensity over all annuli of the disk one can find the total flux of the disk and from there the total energy density of the disk per frequency. This then needs to be scaled to incorporate the location of our emitting region which sits at a distance R from the accretion disk.

The resulting spectral energy density is then given by

$$U_d(\nu) = \frac{2\pi}{c} \int_{\mu_d}^1 I(\nu) d\mu \quad (13)$$

where μ_d is the cosine of the angle between the location on the disk and the normal of the disk with respect to and observer.

X-ray corona: The photon field from the x-ray corona is assumed to be a power law spectrum with a cut off at high energies. Its total energy emitted is related to the disk Luminosity by the equation $L_{cor} = fL_d$ where f is the fraction of the disk luminosity that is emitted by the corona. The spectral energy density of the corona is then given by

$$U_{cor}(\nu) = D(R) \left(\frac{\nu}{\nu_0} \right)^{-\alpha} \exp \left(-\frac{\nu}{\nu_{cut}} \right) \quad (14)$$

The factor $D(R)$ is a scaling factor that incorporates the position of the observer in similar fashion to the disk. The integral of the spectral energy density over all frequencies should equate to the total energy density in x-ray at the location of the emitting region.

The energy density of x-ray around the central engine is given by a

$$UX(R) = \frac{f_X L_d \Gamma^2}{\pi (R_X)^2 c} \left(1 - \mu_X - \beta(1 - \mu_X^2) + \frac{\beta^2(1 - \mu_X^3)}{3} \right) \quad (15)$$

where

$$\mu_X = \left(1 + \frac{R_X^2}{R^2} \right)^{-0.5}.$$

Here f_X is the fraction of the disk luminosity that is emitted by the x-ray corona, L_d is the disk luminosity, Γ is the lorentz factor of the jet, R_X is the size of the x-ray corona, c is the speed of light, β is the velocity of the observer in units of the speed of light. In short the x-ray energy density stays constant until the observer is further away where it will decrease as $1/R^2$ which is to be expected.

Broad line region: The broad band field is assumed to be emitting a black body spectrum as in 12 which peaks at the Lyman-alpha line. The Lyman-alpha line is a spectral line of hydrogen when the atomic electron transitions from the $n = 2$ to the $n = 1$ orbital corresponding to a frequency of $\nu_\alpha = 2.47 \times 10^{15}$ Hz. Similarly to the x-ray corona the spectral energy density is scaled to the region of interest and the total energy density is given by:

$$UBLR(R) = \begin{cases} \frac{f_{BLR} L_d \Gamma^2}{\pi R_{BLR}^2 c} & \text{if } R \leq R_{BLR}, \\ \frac{f_{BLR} L_d \Gamma^2}{\pi R_{BLR}^2 c \beta^3} [2(1 - \beta \mu_{IR1})^3 - (1 - \beta \mu_{IR2})^3 - (1 - \beta)^3] & \text{if } R \geq 3R_{BLR}, \\ aR^b & \text{otherwise,} \end{cases} \quad (16)$$

where

$$\mu_{IR1} = \left(1 + \frac{R_{BLR}^2}{R^2} \right)^{-0.5},$$

$$\mu_{IR2} = \left(1 - \frac{R_{BLR}^2}{R^2} \right)^{-0.5},$$

Parameter	Value
L_d	10^{43} erg/s
GM	$G10^8 M_\odot$
RS	$\frac{2GM}{c^2}$
η	0.1
f_X	0.3
R_X	$30RS$
β	$0.4 c$
f_{BLR}	0.1
R_{BLR}	$10^{17} \sqrt{L_d/10^{45}} \text{ cm}$
f_{IR}	0.5
R_{IR}	$2.510^{18} \sqrt{L_d/10^{45}} \text{ cm}$
Γ	1.1

Table 1: Parameters used to determine the SED of the different regions.

Torus: There is also assumed to be a dusty torus around the AGN emitting in infrared. The spectral energy density of the torus is also given by a black body spectrum with the temperature of the torus being set at $T_{\text{IR}} = 370 \text{ K}$. The total energy density of the torus has the same relations as equation 16 but with the relevant parameters for the torus.

$$\text{UIR}(R) = \begin{cases} \frac{f_{\text{IR}} L_d \Gamma^2}{R_{\text{IR}}^2 c} & \text{if } R \leq R_{\text{IR}}, \end{cases} \quad (17)$$

Total energy density

The total energy density of the photon fields as a function of distance is then seen in figure 1. Here one can see that the energy density of the photon fields is constant until the observer is outside the size of the respective regions. From the image it is clear that the biggest contributor to the total energy density becomes the IR torus, but all the regions contribute significantly to the total energy density.

Spectral energy density

The spectral energy density of the different regions is of more interest since this is what will determine the effect of pion decay on protons accelerate in the jet or in the lobes. To create the SED one has estimated the dynamical scale of our system and used the total photon densities to scale the SED accordingly. The resulting SED is seen in figure 2. The SED are determined also on a number of parameters, all which have taken from the literature. They are seen in table 1.

The choice of variables comes from three sources. Bronzini et al. 2024 and Kiehlmann et al. 2023 which both gives the disk luminosity of CSOs sources, and which we set to 10^{43} erg/s . Ghisellini and Tavecchio 2009 gives the rest of parameters that relate the different regions to the disk luminosity. The biggest caveat here is that these parameters are not specific to CSOs, but to Blazars in which they are based. For the purposes of this analysis one assumes that the parameters are the same for CSOs as for Blazars, and that one would not expect any significant difference.

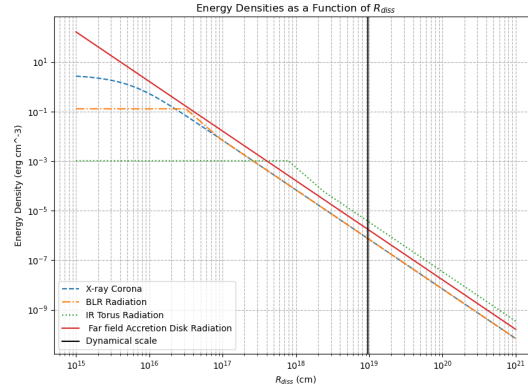


Figure 1: The total energy density of the photon fields as a function radius from central engine.

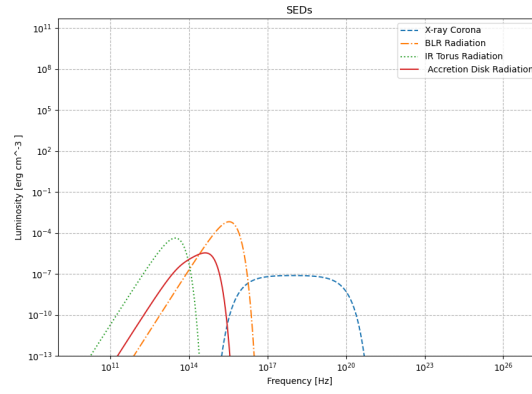


Figure 2: The spectral energy density at distance R

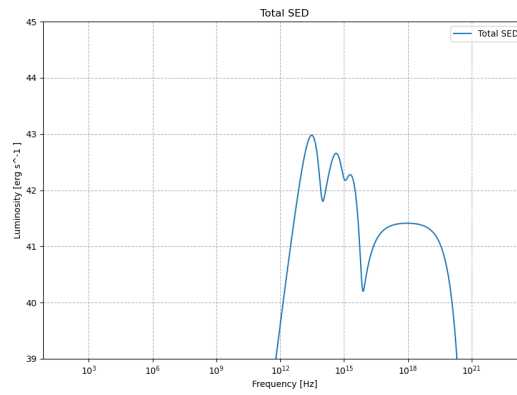


Figure 3: Luminosity of the different components of the CSO that are close by the central engine. Missing synchrotron and IC part which is most prominent

3.3 Classification of CSO

From the papers of Kiehlmann et al. 2023 to Readhead et al. 2023, and from Sullivan et al. 2024 there is a clear quite new classification of CSOs. The classification is based on firstly CSOs being edge brightened or edge dimmed. Edge brightened sources which will onwards be referred as CSO 2s are bright in radio in their lobes, and CSO 1s or edge dimmed are thought to be CSOs that have stalled.

The big picture on CSOs is that they are a group of very short-lived sources that are ignited by transient events. Saying if the ignition of their jets are due to transient event such as tidal disruption event are covered in Sullivan et al. 2024 and for the purposes of this study not necessary to discuss, but start a very interesting conversation. CSOs are then symmetric with the expansion of their jets into the interstellar medium visible from radio telescope. The symmetry of the jets is a key feature of CSOs and makes them unique in the sense of jetted-AGN since they have little to no features of relativistic beaming.

Stability in jet expansion and lobes. The most promising feature of CSOs which we will see as a key feature in the section on time-scales is the stability of the lobes in radio emission and the stability of the jet expansion and the stability of most wavelengths in emissions. In Bronzini et al. 2024 they report no significant variability of one CSO source in gamma rays, variability of the order of years in x-ray, with the broadband SED showing variability on the timescales of years. This is a clear distinction from other jetted AGN which are known to be highly variable.

References

- Balasubramaniam, K. et al. (Nov. 2021). “X-Ray Emission of the gamma-ray-loud Young Radio Galaxy NGC 3894”. In: *The Astrophysical Journal* 922.1, p. 84. ISSN: 1538-4357. DOI: 10.3847/1538-4357/ac1ff5. URL: <http://dx.doi.org/10.3847/1538-4357/ac1ff5>.
- Bronzini, E. et al. (2024). *Investigating X-ray Emission in the GeV-emitting Compact Symmetric Objects PKS 1718-649 and TXS 1146+596*. arXiv: 2401.16479 [astro-ph.HE].
- Ghisellini, G. and F. Tavecchio (Aug. 2009). “Canonical high-power blazars”. In: *Monthly Notices of the Royal Astronomical Society* 397.2, pp. 985–1002. ISSN: 1365-2966. DOI: 10.1111/j.1365-2966.2009.15007.x. URL: <http://dx.doi.org/10.1111/j.1365-2966.2009.15007.x>.
- Hogg, David W. (2000). *Distance measures in cosmology*. arXiv: astro-ph/9905116 [astro-ph].
- Kiehlmann, S. et al. (2023). *Compact Symmetric Objects – I Towards a Comprehensive Bona Fide Catalog*. arXiv: 2303.11357 [astro-ph.HE].
- Readhead, A. C. S. et al. (2023). *Compact Symmetric Objects – III Evolution of the High-Luminosity Branch and a Possible Connection with Tidal Disruption Events*. arXiv: 2303.11361 [astro-ph.HE].
- Sullivan, Andrew G. et al. (2024). *Small-scale radio jets and tidal disruption events: A theory of high-luminosity compact symmetric objects*. arXiv: 2401.14399 [astro-ph.HE].